

# NATIONAL ADVISORY COMMITTEE FOR AERONAUTICS

TECHNICAL NOTE 3880

MEASUREMENTS OF LIFT FLUCTUATIONS DUE TO TURBULENCE

By P. Lamson

California Institute of Technology



Washington

March 1957





0067092

## NATIONAL ADVISORY COMMITTEE FOR AERONAUTICS

## TECHNICAL NOTE 3880

## MEASUREMENTS OF LIFT FLUCTUATIONS DUE TO TURBULENCE

By P. Lamson

## SUMMARY

The fluctuating lift of a rigid wing in turbulent flow was studied and the power spectra of the lift and of the turbulent fluctuations were measured. From these measurements the aerodynamic admittance of the wing was obtained. The ratio of span to scale of turbulence was varied by means of movable end plates. For a distance between the end plates of the order of the scale of turbulence the aerodynamic admittance is expected to approach the computed values of Sears. This is shown to be the case if the reduced frequencies  $k$  are larger than  $k = 0.8$ . For smaller values of  $k$  the experimental admittance falls below Sears' values. For large ratios of span to scale of turbulence the aerodynamic admittance is decreased for all frequencies and becomes nearly independent of frequency in the investigated range  $0.2 \leq k \leq 2$ .

In general, the measurements support the simplifying assumptions made in the statistical approach to gust loads and buffeting initiated by Clementson and by Liepmann.

## INTRODUCTION

The lift and drag of a wing or of a whole configuration are usually computed on the basis of a known flight velocity  $U$  and a known angle-of-attack distribution  $\alpha$ . In every practical case there will exist, however, random fluctuations, which may be termed "noise," both in  $U$  and  $\alpha$ .

For a rigid configuration these fluctuations are due to turbulence which may be present in the atmosphere or produced by part of the airplane itself. The first case deals with flight through a gusty atmosphere; the second case, with buffeting. Both problems belong to a class of phenomena in which a mechanical system is excited by random forces. In the case of interest here,  $U$  and  $\alpha$  are the "input"; lift, drag, or any other defined mechanical response of the airplane are considered the "output" or "response."

To make the problem tractable without losing its significant physical character it may be assumed that the noise is statistically stationary,

that is, that it has statistical properties which are independent of time when averaged over a time which is long compared with a characteristic time of the particular response. For example, for a particular mode of wing bending the characteristic time is the time which enters into the logarithmic decrement of the oscillation. Furthermore, the problem is linearized; that is, the relation between force and response is considered linear. Hence, the input is restricted to small fluctuations. This assumption is usually well satisfied.

The problem of finding the response of a linear system with statistically stationary forces is now considered. Such a problem can be handled with generalized harmonic analysis. One can introduce power spectra for the input and output and use the concepts of admittance, impedance, or transfer function to characterize the system. For a given input spectrum and known system, the output spectrum and, hence, the mean square of the output can be obtained easily.

These concepts were first applied to aerodynamical problems by Clementson (ref. 1) and Liepmann (ref. 2) independently. Since then a large number of papers have dealt with various aspects of the problem (e.g., refs. 3, 4, and 5). In the first papers the problem was considered as a one-dimensional stochastic process (i.e., the angle of attack was considered a random function of time only and spatial variation of  $\alpha$  was neglected). The response of the configuration was described by a simple transfer function. Recently, the theory has been extended to fluctuations which, like actual turbulence, vary in space and time (i.e., at any given time the fluctuations are not uniform along the span), and account has been taken of the finite span of the wing (refs. 4 and 6).

The most interesting part of the admittance or transfer function of a wing is the aerodynamic admittance. This aerodynamic admittance relates the angle of attack of a rigid airfoil to the lift. This relation varies with frequency because of the loss of lift due to circulation lag. In reference 2 Sears' result (ref. 7) for the aerodynamic admittance (for a sinusoidal input) was used to demonstrate the character of the response.

The present experimental investigation was undertaken to study in detail a basic problem in this field, namely, the lift of a rigid wing in turbulent air.

Thus, the fluctuating lift of a wing in an airstream with known turbulence was measured and analyzed. The results can be compared with the theoretical studies cited above. The experiments are necessary to check on the validity of some of the simplifying assumptions made in the theory. Furthermore, the experiments demonstrate the possibility of measuring aerodynamic transfer functions from a study of the response of a configuration in a field of turbulence. There is little doubt that this technique will become very useful in flight testing.

The investigation was carried out at the California Institute of Technology under the sponsorship and with the financial assistance of the National Advisory Committee for Aeronautics.

The author wishes to acknowledge the guidance of Professor H. W. Liepmann and the help of Dr. G. T. Skinner.

## SYMBOLS

A	area under square of mechanical-admittance curve
$A_r$	aspect ratio
B	strength of magnet
$C_L$	lift coefficient
$C_{L_\alpha}$	lift-curve slope
c	chord
F	force
$f(\omega)$	angle-of-attack spectrum
G	spring constant
$g(\omega)$	lift spectrum
$h(\omega)$	displacement spectrum
I	current in coil
k	reduced frequency, $\omega c/2U$
L	lift
M	mesh size
m	mass
$R_e$	Reynolds number
s	span of wing

$T$	time scale
$t$	time
$t_s$	span of movable strip
$U$	mean air velocity
$u$	component of fluctuating turbulent velocity in direction of free stream
$v$	displacement
$w$	component of fluctuating turbulent velocity in direction of lift vector
$x$	distance downstream of turbulence grid
$y$	spanwise coordinate
$\alpha$	angle of attack
$\beta$	viscous damping constant
$\zeta$	autocorrelation
$\theta$	angle hot-wire anemometer makes with free stream
$\lambda_x$	scale of turbulence in free-stream direction
$\nu$	oscillatory frequency, cps
$\nu_0$	natural oscillatory frequency
$\nu_s$	shedding frequency of cylinder
$\tau$	time delay (used in defining autocorrelation, appendix A)
$\phi$	aerodynamic admittance
$\chi$	total admittance
$\psi$	mechanical admittance
$\omega$	circular frequency
$\omega_0$	natural circular frequency

## DEFINITIONS AND MEASURING PRINCIPLES

It has been pointed out that the random nature of the problem allows application of the ideas of stationary stochastic processes. Therefore, it is desirable to measure some of the statistical quantities which define such a process. Specifically, the quantities measured are the turbulence spectrum, the airfoil displacement spectrum, the lift-curve slope of the airfoil, and the mechanical admittance (frequency response) of the spring system. From these measurements one may find the lift spectrum and the aerodynamic admittance.

## Aerodynamic Admittance

For a linear system under stochastic forcing the ratio of the response spectrum to the input spectrum is equal to the absolute square of the admittance. For the case of an airfoil in a turbulent stream, the lift may be regarded as the response and the fluctuating angle of attack presented by the turbulent stream as the input. The square of the aerodynamic admittance is then equal to the ratio of lift spectrum  $g(\omega)$  to angle-of-attack spectrum  $f(\omega)$ . The mean-square lift  $\overline{L^2}$  and the mean-square angle of attack  $\overline{\alpha^2}$  are thus expressed by

$$\overline{\alpha^2} = \int_0^{\infty} f(\omega) d\omega$$

$$\overline{L^2} = \int_0^{\infty} g(\omega) d\omega$$

If  $\phi(\omega)$  denotes the complex aerodynamic admittance then  $|\phi|^2$  is related to  $f(\omega)$  and  $g(\omega)$  by

$$g(\omega) = |\phi|^2 f(\omega) \quad (1)$$

## Turbulence Spectrum

If  $w$  denotes the component of fluctuating turbulent velocity in the direction of the lift vector, then the fluctuating angle of attack is given approximately by  $\alpha(t) = \frac{w}{U}$ . The  $w$  spectrum of turbulence is measured by putting the output from a  $w$  sensitive hot-wire anemometer into a wave analyzer.

### Lift Spectrum

The lift spectrum must be found indirectly, since in the experiment only the displacement of the airfoil is measured. The lift spectrum  $g(\omega)$  and displacement spectrum  $h(\omega)$  are again related by the mechanical admittance of the spring system which supports the airfoil. The mean-square displacement  $\overline{v^2}$  is given by

$$\overline{v^2} = \int_0^{\infty} h(\omega) d\omega$$

If the mechanical admittance is denoted by  $\psi(\omega)$  then

$$h(\omega) = |\psi|^2 g(\omega) \quad (2)$$

The displacement spectrum is measured by putting the voltage output from a displacement pickup into a wave analyzer. The mechanical admittance is found by measuring the displacements which result when the airfoil is driven sinusoidally by means of a coil and magnet at frequencies selected by an oscillator.

### Total Admittance

The measured quantities are the mechanical admittance  $\psi$ , the displacement spectrum  $h(\omega)$ , and the angle-of-attack spectrum  $f(\omega)$ . The aerodynamic admittance is to be obtained from this information. The above spectra are related by some total admittance  $\chi$ , such that

$$h(\omega) = |\chi|^2 f(\omega) \quad (3)$$

As seen from equations (1), (2), and (3), the total admittance  $\chi$  is just the product of mechanical admittance and aerodynamic admittance as shown by

$$h(\omega) = |\phi|^2 |\psi|^2 f(\omega) \quad (4)$$

therefore,

$$|\chi|^2 = |\phi|^2 |\psi|^2$$

Therefore, the absolute aerodynamic admittance  $|\phi|$  is found from the measured quantities

$$|\phi| = \frac{1}{|\psi|} \left[ \frac{h(\omega)}{f(\omega)} \right]^{1/2} \quad (5)$$

### Finite-Span Effect

To determine experimentally the effects of finite span, the span has been made adjustable by means of sliding end plates (fig. 1). The maximum span is fixed by the spanwise dimension of the wind-tunnel jet. The minimum span is limited as a consequence of the fact that, since forces are found from displacements, at least a portion of the airfoil must undergo displacement. If the movable portion is a narrow strip of the span then the strip width is the minimum span that can be obtained. This is because the end plates cannot be brought closer together than the strip width without interfering with the motion of the strip.

Several considerations limit the strip width. The strip width must be large enough so that (1) the aerodynamic forces are adequate for measurement and (2) the gap effects are small. The strip width should be small enough so that the minimum-span position approximates the limiting case of two-dimensional turbulence over the strip. If the minimum span is less than the scale of turbulence, three-dimensional effects are sufficiently small so that the two-dimensional case is approximated.

## EXPERIMENTAL EQUIPMENT AND PROCEDURES

### Wind Tunnel

The wind tunnel used for the experiments is a low-speed tunnel which opens into a free jet at the working section. The original jet size of 7 by 72 inches has been reduced to 7 by 12 inches in order to increase the maximum velocity. With a turbulence grid in the contraction section the maximum speed is about 65 mph; without the grid the maximum speed is about 100 mph.

### Model Airfoil

The airfoil tested has a 20-percent-thick symmetrical section and a  $2\frac{1}{2}$ -inch chord. Only a narrow strip (0.7 inch in span) of the airfoil is movable. The floating strip is located at midspan as shown in figure 2.

The small size of chord was chosen for several reasons. First, the jet is small and consequently the model must be small if tunnel-wall corrections are to be kept small. Second, the theory assumes that the turbulence pattern does not change as the air passes over the chord. This requirement can be approximated only if the chord is small compared with the distance over which significant turbulent decay takes place. Finally, to obtain adequate response the chord should not be large compared with the scale of turbulence, and the scale of turbulence is limited by the jet dimensions and the grid size.

### Force Measurements

Because of the small size of the airfoil it did not seem feasible to measure forces by means of pressure pickups. Therefore, it was decided to find forces from displacement measurements. The floating strip, upon which forces are to be found, must be constrained to small displacements if a rigid airfoil is to be simulated. Consequently, the floating strip is supported by a relatively stiff spring system. Because of the small size of the airfoil there was not space to mount supporting springs next to the strip, so it was necessary to put the spring system outside the airfoil (figs. 2 and 3). A beam, whose stiffness is much greater than that of the supporting springs, carries the load from the floating element to the springs. The beam lies inside a slot in the fixed dummy airfoil. The spring system consists of parallel flexure links which constrain the motion to simple plunging.

### Pickup

The displacement pickup is a small differential transformer (Schaevitz gage). Exciter current of 100 kilocycles, supplied to the transformer coil by a crystal oscillator, is modulated by an iron core which moves with the airfoil (fig. 2). The modulated signal is then demodulated and put into a wave analyzer, filter, or integrator.

### Spectrum Measurements

Three frequency ranges may be distinguished according to the instrument used for the spectrum measurements. Above approximately 70 cps a Hewlett-Packard wave analyzer is used. A Krohn-Hite low pass filter covers the frequency range from 2 to 10 cps. Spectrum points between 10 and 70 cps may be found by using the mechanical resonance of the airfoil

spring system as the filter. This latter method is discussed in detail in a subsequent section.

### Integrator

The large fluctuations of the response make it necessary to use some kind of integrator in order that some average root-mean-square value can be obtained. For this purpose a resistance-capacitance circuit with a time constant of  $17\frac{1}{2}$  minutes is used. Measurements of total response require about a 10-minute averaging time to get less than 5-percent scatter.

### Mechanical Admittance

It was at first believed that the mechanical admittance could be computed by assuming the spring system to be a one-degree-of-freedom damped oscillator. The motion would then be described by the equation

$$m\ddot{v} + \beta\dot{v} + Gv = F(t)$$

and the absolute admittance would be given by

$$|\psi| = \frac{1}{\left[ m^2(\omega^2 - \omega_0^2)^2 + \beta^2\omega^2 \right]^{1/2}}$$

This simplified picture proved to be inadequate because, in addition to the natural frequency of the parallel link system, a mode of oscillation involving the beam in bending appeared in the response spectrum. Therefore, it seemed necessary to find the mechanical admittance experimentally.

The mechanical admittance is found by measuring the displacement as a function of frequency for a driving force of constant amplitude. For this purpose a coil carrying an amplified oscillator signal is attached rigidly to the end of the beam. The coil lies in the field of a permanent magnet of strength  $B$ , so that the force exerted on the coil when it carries current  $I$  is just  $\vec{F} = \vec{B} \times \vec{I}$  (if the frequency is not too high).

Details of the arrangement are shown in figure 3. The coil is aligned in the circular air gap of the magnet by means of a cylindrical spacer which is pulled out of the gap when the cement which bonds the coil to the beam has set.

To find the point at zero frequency, direct current is put through the coil. The point at zero frequency is essential because one wants to compare the dynamic response of the airfoil at each frequency to the static lift of the airfoil.

### Lift-Curve Slope

Since for admittance measurements the dynamic response at each frequency is referred to the static lift of the airfoil, the lift-curve slope is measured. This is done by rotating the airfoil in the flow. The force measured is actually the normal force but this force is very nearly equal to the lift for small angles of attack. The lift-curve slope is measured with the grid in the tunnel, since without the grid the slope is about 20 percent larger and also laminar separation causes the lift curve to bend over at about  $60^\circ$ . The lift-curve slope of the airfoil is about 4 per radian. No appreciable change with Reynolds number occurs for the range of Reynolds number considered (approximately 80,000 to 150,000). The lift curve is plotted in figure 4.

### Selection of Spring Stiffness

The parallel flexure links, which comprise the spring system, must be stiff enough to restrict the motion to small displacements in order that (1) the airfoil motion will not modify the flow field and (2) the aerodynamic damping will be small. An instrument which is capable of measuring sufficiently small displacements (fluctuating or static) is the Schaevitz gage. The Schaevitz gage instrumentation is designed to allow a maximum displacement of 0.004 inch in low-sensitivity position and a maximum displacement of 0.001 inch in high-sensitivity position. In selecting the spring stiffness the maximum linear range of the pickup determines the upper limit of deflection, whereas the signal-to-noise ratio determines the lower limit.

For design purposes it is satisfactory to assume a one-degree-of-freedom system as  $m\ddot{v} + \beta\dot{v} + Gv = F(t)$ . Now, consider how much each parameter can be varied. A minimum mass is fixed by the spring-beam arrangement shown in figure 2. If no artificial damping is introduced, the structural damping of the flexure links is the definitive damping of the system. An estimate of the forces can be obtained from the theory. From the above information a fair guess can be made of suitable values of spring constant  $G$ . The dimensions of the flexures which will give this spring constant can then be computed.

### Turbulence Spectrum

Turbulence is created in the airstream by means of a grid upstream of the airfoil. To find the fluctuating angle of attack which the airfoil experiences because of the turbulent stream one must find the velocity fluctuations in the direction of the lift vector. Denoting this velocity component of the turbulence by  $w$  and the mean speed by  $U$  gives, for small values of  $w$  compared with those of  $U$ ,

$$\alpha(t) = \frac{w}{U}$$

The component  $w$  is measured by hot-wire anemometry. Two hot-wires are placed close together in the flow, so that both wires lie in planes parallel to the plane of  $w$  and  $U$ . The resistance of a hot-wire and consequently of the voltage across it is a function of wire temperature. The wire temperature depends upon the component of velocity normal to the wire. Hence, if one wire is at angle  $\theta$  ( $\theta = 45^\circ$  and  $\theta = 60^\circ$  were both used) and the other is at  $-\theta$  to the free-stream direction, each wire will have the same voltage drop so that the voltage difference between the two wires will be zero. Thus, this configuration of hot-wires is sensitive to only the  $w$  velocity component. The  $w$  meter may be calibrated either by rotation in a uniform stream, recording voltage difference as a function of angle, or by comparison with standard turbulence grids.

The wires used were 1/10-mil platinum-rhodium wire and 1/20-mil platinum wire. There are several advantages in using such fine wires. First, the time constant is sufficiently short so that no compensation for thermal lag is necessary over the range of frequencies considered. Also, the sensitivity of the fine wires is large enough so that the signal can be put directly into a wave analyzer. No preamplification is needed so one source of noise is eliminated. A disadvantage of using very fine wires, especially 1/20-mil platinum, is that they are easily broken or bent out of shape by dust particles in the flow. The  $w$  meter is calibrated before and after each run to determine if the wires have been bent during the run.

Two different grids were used in order to vary the scale of turbulence. The small grid is made of 1/4-inch-diameter wooden dowel rod with horizontal rods spaced 1 inch apart and vertical rods spaced 1 inch apart (i.e., mesh size  $M$  equals 1). The large grid is of 1/2-inch-diameter dowel with horizontal rods spaced 3 inches apart and vertical rods spaced 2 inches apart.

The scale of turbulence is found from the intercept of the  $u$  spectrum of turbulence ( $u$  being the fluctuating component of velocity in the stream direction) as shown in appendix A. For the small grid the scale is  $\lambda_x \approx 1/2$  inch and for the large grid,  $\lambda_x \approx 1$  inch.

### Spring System as Mechanical Filter

The resonance peak of the undamped spring system is so sharp that nearly all of the area under the mechanical-admittance curve is contained within a frequency range of a few cycles (fig. 5). This fact suggests the possibility of using the spring system as a mechanical filter. The mean-square displacement  $\bar{v}^2$  is given by integration of equation (4) over all frequencies

$$\bar{v}^2 = \int_0^{\infty} h(\omega) d\omega = \int_0^{\infty} |\phi|^2 |\psi|^2 f(\omega) d\omega \quad (6)$$

where  $\psi$  is the mechanical admittance and  $\phi$  the aerodynamic admittance. Since  $\psi$  has a sharp peak at the natural frequency  $\omega_0$ , whereas  $\phi$  and  $f(\omega)$  are comparatively slowly varying functions, one may write

$$\bar{v}^2 \approx |\phi(\omega_0)|^2 f(\omega_0) \int_0^{\infty} |\psi|^2 d\omega$$

Hence, to find the absolute aerodynamic admittance  $|\phi(\omega_0)|$ , one measures the total response  $\bar{v}^2$ , the turbulence spectrum at  $\omega_0$ , and  $f(\omega_0)$  and computes the area  $A$  under the square of the mechanical-admittance

curve  $\int_0^{\infty} |\psi|^2 d\omega = A$ .

Then (see appendix B, method I),

$$\begin{aligned} \sqrt{\bar{v}^2} &= |\phi(\omega_0)| \sqrt{f(\omega_0)A} \\ |\phi(\omega_0)| &= \sqrt{\frac{\bar{v}^2}{f(\omega_0)A}} \end{aligned} \quad (7)$$

### Hewlett-Packard Wave Analyzer

The turbulence spectrum above 30 cps and the displacement spectrum above about 70 cps are measured on a Hewlett-Packard model-200A harmonic-wave analyzer. This analyzer has an adjustable half-band width from 30 to 145 cps where the half-band width is defined as the number of cycles off resonance at which a given signal is attenuated 40 decibels. Only the 30-cps half-band width is used, since only comparatively low frequencies

are of interest. Measurements of the displacement spectrum could not be made to as low a frequency as were those for the turbulence spectrum because the turbulence spectrum is quite flat at the low-frequency part of the spectrum while the displacement spectrum has a sharp peak (at the natural frequency). Since, in measuring a continuous spectrum with the analyzer, one assumes that the spectrum is flat or at least linear over the pass band of the analyzer, points of the displacement spectrum may be obtained only so long as the analyzer pass band does not include a portion of the spectrum which has large curvature (such as occurs when the band width overlaps the resonance peak). For example, the displacement spectrum for the spring system whose natural frequency is 34 cps is sufficiently flat at frequencies above about 70 cps to allow accurate spectrum measurement with a 30-cps half-band width. A sample calculation is given in appendix B, method II.

The displacement spectrum is not found for frequencies higher than about 200 cps because the ratio of noise (i.e., extraneous vibrations) to signal is no longer small above 200 cps.

#### Low-Band-Pass Filter

As previously discussed, the Hewlett-Packard wave analyzer covers the high-frequency end of the spectrum and the spring system used as a mechanical filter measures spectral points in the range of 10 to 70 cps. To obtain low-frequency points (2 to 10 cps) a Krohn-Hite low-band-pass filter is used. The filter pass band can be adjusted to any width by means of independently controlled high- and low-frequency cutoffs. Once a particular band width has been selected, the shape of the pass band may be found by putting an oscillator signal into the filter and varying the frequency while holding the amplitude constant. However, to find the admittance, only the ratio of input to response is needed, so that by using the same pass band for input and response the area under the pass band is divided out and, hence, does not enter in the admittance computation.

#### Second Spring System

For a number of reasons it was decided that a new spring system could be designed which would have many advantages over the old system (of fig. 2). The main difficulty encountered with the original system is the instability of the mechanical admittance. The instability is presumably caused by the flexure links being built up from pieces so that some slippage occasionally occurs during vibration at the interfaces of the metal pieces. As a result end-fixity conditions are changed and a shift occurs in the natural frequencies of the system. Figure 6 illustrates the effect of the frequency shift on the admittance curve. It is

noted that a small shift can introduce a large change in the amplitude at any particular frequency. Also, a change in the area under the curve usually accompanies the frequency shift. As discussed previously, the use of the mechanical system as a filter involves the area under the admittance curve so that this area should remain constant. In the new system (fig. 3) frequency instabilities are overcome by machining each flexure link from a single piece of metal. In using the spring system as a filter the natural frequency picks out a single spectral component. Hence, it is desirable to vary the natural frequency in order to obtain other spectral points. Therefore, three sets of flexures were made giving natural frequencies of 17, 34, and 68 cps. Intermediate frequencies can be found by screwing threaded brass weights into the hole at the beam center of gravity as shown in figure 3. Also, the different maximum amplitudes of deflection which result from the different spring stiffnesses allow the study of aerodynamic damping as a function of airfoil motion.

The symmetry of the new system serves several purposes. First, the amplitude of the mode of oscillation involving the beam in bending is less for a symmetrical system. Second, the mechanical admittance obtained by an input at one end of the beam is approximately the same as if the input were applied at the other end of the beam. Therefore, one can mount the driving coil at one end of the beam and the strip of airfoil at the other end. This arrangement is a great convenience since the driving unit does not have to be disassembled and reassembled each time one wants to calibrate (i.e., find mechanical admittance). A disadvantage lies in the fact that sometimes a small metal chip gets lodged between magnet and coil during a run, but this can be discovered by calibrating before and after each run.

#### Vortex-Street Input

As a first step toward a study of the response of an airfoil to a turbulent airstream, it seemed instructive to find the response to a sinusoidal input, since the results could then be compared with the results of Sears' theory for a rigid airfoil in a sinusoidal gust. To simulate a sinusoidal gust a vortex street was formed by means of a large cylinder upstream of the airfoil. Unfortunately, no wake position could be found for which there was not considerable background turbulence, and, consequently, a whole spectrum of frequencies was excited. If the street is made small enough so that no background turbulence appears then it is of insufficient strength to excite the airfoil. One might also ask if the shedding frequency could be brought into coincidence with the natural frequency of the spring system, thereby making the response to the vortex street essentially the entire response. Due to the sharpness of the peaks this condition of coincidence is too critical to allow accurate measurement. An example of the displacement spectrum obtained for the airfoil in the wake of a cylinder is shown in figure 7.

### Secondary Flow

When the end plates were initially placed one on either side of the movable strip of airfoil, the aerodynamic admittance was found to be larger than 1 as the frequency approached zero. The lift as the frequency tends to zero may be less than the static lift (because the angle-of-attack correlation along the span may be less than 1) but it cannot exceed the static lift. To explain this difficulty it was assumed that some kind of secondary flow occurred between the plates which caused the dynamic response of the airfoil to be too high. A tuft placed in the flow between the plates illustrated that the flow was at least separating rather badly. Fillets were then added at the intersection of plate and airfoil as shown in figure 1. Again, the tuft was placed in the flow and this time no evidence of separation could be found.

### Gap Effect

To determine the effect of the gaps on either side of the movable strip of airfoil, measurements of the response were made with the gaps covered by microfilm. The film was found to restrain the motion of the strip so that it was necessary to apply the film with the gaps enlarged to about 1/4 inch and then to buckle the film by restoring the gaps to their original width of a few hundredths of an inch. This meant that some end effects would still be present because of the grooves formed by the buckled film, but at least air could not pass through the gaps. The static lift-curve slope and the dynamic response of the airfoil were found to be (within the error of measurement) the same as they were without the film.

### Noise Level

To find how much of a given response measurement is due to extraneous vibrations from the test stand and electrical noise in the instrumentation, the movable strip of airfoil is shielded from the flow. The overall noise level is then simply the shielded reading. The shield is a hollow airfoil section which is large enough to clear the strip airfoil as shown in figure 8. The noise level was negligible for the measurements reported here.

### Damping

It is desirable to vary the damping of the spring system for several reasons. First, in actual flight conditions the vibrating structure might be predominately damped by either structural damping or aerodynamic damping so that both cases deserve investigation. Second, since the linear range of the Schaevitz gage must simultaneously accommodate amplitudes corresponding to a whole spectrum of displacements, the largest amplitude (i.e.,

resonance peak) should not be too large compared with the smallest amplitude considered (corresponding to some arbitrary frequency  $v_{\max}$ ). This is illustrated in figure 9.

Damping by means of an oil-filled dashpot was attempted but was unsuccessful since the velocities are too small to be appreciably influenced by this kind of damping. Then, an attempt was made to increase the structural damping by painting a rubber compound on the flexure links at the grooves where the bending takes place. The system could be almost critically damped in this way but the deflection was no longer linearly related to the force (at a given frequency).

Finally, damping by means of a rubber strip in tension was tried. The force-deflection linearity was restored but some additional modes of vibration appeared which were not very reproducible. Consequently, all the data presented are for the undamped system. It is felt, however, that a damped system could be made to work if more time were spent on the problem.

Aerodynamic damping of the airfoil motion was too small to show up in the admittance in all measurements except in those involving the largest amplitude of motion, that is, for the case of the mechanical filter using the weakest springs. For this case the admittance (figs. 10(a) and 10(b),  $k \approx 0.1$  to  $0.3$ ) in general drops somewhat below the curve drawn through the other points. That the effect is more pronounced with increasing mean speed (and, hence, with increasing displacement amplitude) suggests that aerodynamic damping is the cause.

To check this supposition the mechanical admittance was measured (using the setup shown in fig. 3) with and without a free stream. The mechanical admittance when measured in the free stream was not diminished enough to account for the effect mentioned above; however, the method of accounting for the aerodynamic damping by calibration is not quite comparable to the actual situation existing in the response to a turbulent flow, since in the former case the driving force is applied at one end of the beam and the damping force at the other, whereas in the latter case all forces are applied at one end of the beam.

## RESULTS

### Infinite Wing

The essential results of the measurements for an infinite wing are plotted in figures 10(a) and 10(b). Two sets of data are given in each figure, one for the wing with end plates and the other for the wing spanning the jet. The distance between end plates is small enough so

that the turbulent fluctuations are nearly correlated across the effective span and, hence, these sets of data should agree with the admittance function from Sears' theory. This is seen to be true for reduced frequencies larger than about 0.8. For smaller reduced frequencies the measured admittance is well below Sears' curve. This effect is more pronounced for the large grid (fig. 10(b)).

Two reasons are suggested to explain this effect. One is the inhomogeneity of the turbulence at low frequencies. The effect is more pronounced for the large grid because the airfoil is effectively closer to it ( $x/M = 8$  for the large grid, whereas  $x/M = 20$  for the small grid). A few tentative measurements using the small grid at  $x/M = 8$  support this conjecture.

The other reason is that the end plates may not have been large enough (compared with the large eddies that correspond to low frequencies) to isolate completely the portion of the span between the end plates from the downwash effects due to the wake arising from the rest of the wing. The data of Hakkinen and Richardson (ref. 8) and Richardson (ref. 9) are for an essentially infinite end-plate size (wing spanning a closed tunnel), and dropoff of the admittance curve at low frequencies does not appear.

For the case of the wing spanning the jet it is seen that the entire admittance curve falls far below the Sears' values, indicating that three-dimensional effects are very important and that the two-dimensional admittance function is no longer even approximately valid. The admittance for this case (span large compared with scale of turbulence) is almost independent of frequency, at least within a range of reduced frequencies from 0.2 to 2.0, the highest value for which data were taken. It should be emphasized that simply having the span of the movable strip  $t_s$  less than the scale of turbulence  $\lambda_x$  is not sufficient if one is to measure a two-dimensional aerodynamic admittance. The ratio of total span  $s$  to scale  $\lambda_x$  will always enter.

To clarify the nature of the three-dimensional effects assume the general problem (in which the turbulence presents an angle of attack  $\alpha = \alpha(y, t)$  to the wing) to be composed of two simpler problems, (1)  $\alpha = \alpha(t)$  only and (2)  $\alpha = \alpha(y)$  only. The first case is treated in two-dimensional nonstationary theory (refs. 2 and 7). The second case may be represented by Prandtl's horseshoe-vortex concept in which downwash due to the wake is calculated from the Biot-Savart law. From this consideration of the wake effect it is apparent that, even if the span of the movable strip  $t_s$  is small compared with the scale  $\lambda_x$ , wake effects from the entire span  $s$  will contribute to the response of the strip. This is seen in the experimental data (figs. 10(a) and 10(b)); the large difference in the aerodynamic admittance results from using two

different values of span  $s$  (i.e., with and without end plates) while keeping the scale  $\lambda_x$  and the strip span  $t_s$  fixed.

### Aspect-Ratio Effect

Because of instrumentation difficulties and other unexpected problems arising in the experimental determination of the aerodynamic admittance for a two-dimensional wing, there was little time remaining for investigating the case of a finite-aspect-ratio wing in turbulent flow. However, the few measurements which are discussed below give some indication of the qualitative behavior of the response with changing aspect ratio.

For a constant turbulence level and mean speed, the response of the movable strip for several aspect ratios is given, first, for the strip located near the wing root and, second, for the strip near the wing tip. The relative position of the movable strip and the aspect ratio of the wing may be adjusted by introducing a sliding end plate on the inboard side of the strip and by changing the span of the outboard portion of wing. The portion of wing outboard of the movable strip is supported by two rods which extend from the inboard dummy airfoil through clearance holes in the movable strip to the outboard section.

The static and dynamic response of the strip near the wing root for several configurations is summarized in figure 11. It should be noted that the configuration denoted by  $A_r = \infty$  is of infinite aspect ratio only with regard to tip effects; that is, it is of span  $s$  with regard to the response to turbulence. In figure 11 curve (1) shows that the static response is monotonically diminished because of tip effects as the aspect ratio is decreased. Curves (2) and (3) show that the dynamic response of the root element at first increases as the span is reduced, then decreases. The reason for this is that as the span (and, hence, the wake) is shortened the canceling effect due to the wake is reduced (see section entitled "Infinite Wing"). As the aspect ratio is further reduced the tip effect becomes predominant and causes the response to diminish.

Response of the strip near the wing tip is shown in figure 13. The curves for the tip element show the same trends as those discussed for the root element.

### CONCLUDING REMARKS

The aerodynamic admittance of a wing has been obtained from measurements of the lift power spectrum and turbulence spectrum.

If end plates are used so that the fluctuations are correlated across the effective span of the wing, the physical situation can be made to approximate Liepmann's one-dimensional study. It is then found that the aerodynamic admittance approaches Sears' theoretical curve for reduced frequencies higher than about 0.8. Hence, the assumption made in the theory that the influence of the wing on the turbulence can be neglected is verified by the measurements.

The smoothing effect of a wing span which is large compared with the scale of turbulence is demonstrated. The aerodynamic admittance for the airfoil measured is less by a large factor than that for the case with end plates.

California Institute of Technology,  
Pasadena, Calif., July, 1955.

## APPENDIX A

## SCALE OF TURBULENCE

The scale of turbulence is in a sense an average eddy size as may be seen from the way in which it is defined. One may define a time scale  $T$  of the motion by the area under the autocorrelation curve, where the autocorrelation  $\zeta(\omega)$  is defined by  $\zeta(\omega) = u(t)u(t + \tau)$

$$\zeta(0)T = \int_0^{\infty} \zeta(\tau) d\tau$$

The length scale  $\lambda_x$  is related to  $T$  by

$$\lambda_x = UT$$

so that

$$\lambda_x = U \frac{\int_0^{\infty} \zeta(\tau) d\tau}{\zeta(0)}$$

To write this expression in terms of the power spectrum, one may use the well-known relation

$$f(\omega) = \frac{2}{\pi} \int_0^{\infty} \zeta(\tau) \cos \omega\tau d\tau$$

Therefore,

$$f(0) = \frac{2}{\pi} \int_0^{\infty} \zeta(\tau) d\tau$$

Similarly, from the equation

$$\zeta(\tau) = \int_0^{\infty} f(\omega) \cos \omega\tau d\omega$$

one obtains

$$\zeta(0) = \int_0^{\infty} f(\omega) d\omega$$

Hence,

$$\lambda_x = U \frac{\pi}{2} \frac{f(0)}{\int_0^\infty f(\omega) d\omega}$$

For example, for  $U = 92$  feet per second, the  $u$  spectrum of turbulence for the large grid gives

$$\frac{f(0)}{\int_0^\infty f(\omega) d\omega} = 5.8 \times 10^{-4} \text{ sec}$$

Therefore,

$$\lambda_x = 92 \times \frac{\pi}{2} \times 5.8 \times 10^{-4} = 0.084 \text{ ft}$$

$$\lambda_x \approx 1 \text{ in.}$$

## APPENDIX B

## SAMPLE CALCULATION OF ABSOLUTE AERODYNAMIC ADMITTANCE

## Method I

Using the mechanical system as a filter to find the response at a frequency  $\omega_0$  and the wave analyzer to find the input at this frequency, one may compute the absolute aerodynamic admittance.

At a natural frequency corresponding to  $k = 0.21$ , the root-mean-square response of the airfoil (no end plates) to turbulence created by the large grid is

$$\left(\frac{\overline{v}}{v^2}\right)^{1/2} = 0.18 \text{ volt}$$

At the given airspeed  $U$ , rotation of the airfoil in the flow gives the static calibration

$$\frac{dL}{d\alpha} = 0.10 \text{ volt/deg}$$

so that the response may be put into the units

$$\left(\frac{\overline{v}}{v^2}\right)^{1/2} = 1.8^\circ$$

Similarly, for the input the static calibration consists of rotating the  $w$  meter in the flow

$$[f(\omega_0)]^{1/2} = 0.33^\circ$$

Since input and response are not measured by the same pass band, the pass-band area must be taken into account. Thus, dividing by the 11-cps pass-band area of the Hewlett-Packard Wave Analyzer (corresponding to 30-cps half-band width) gives

$$[f(\omega_0)]^{1/2} = \frac{0.33^\circ}{(11v)^{1/2}} = \frac{0.10^\circ}{v^{1/2}}$$

The area under the square of the mechanical-admittance curve is (fig. 9(b))

$$A = 4,850v$$

Hence, from equation (7),

$$\begin{aligned} |\phi| &= \frac{(\overline{v^2})^{1/2}}{(A)^{1/2}} \frac{1}{[f(\omega_0)]^{1/2}} = \frac{1.8}{(4,850)^{1/2}} \times \frac{1}{0.10} \\ &= 0.26 \end{aligned}$$

at  $k = 0.21$ .

## Method II

Using the Hewlett-Packard wave analyzer to find input and response spectra, one may compute the absolute aerodynamic admittance as shown below. At a reduced frequency  $k = 1.95$  the root-mean-square response of the airfoil (no end plates) to turbulence created by the large grid is

$$[h(\omega)]^{1/2} = 0.010 \text{ volt}$$

By rotating the airfoil in the flow, one obtains the static calibration

$$\frac{dL}{d\alpha} = 0.50 \text{ volt/deg}$$

In order that the response may be put into the same units

$$[h(\omega)]^{1/2} = 0.02^\circ$$

Similarly, for the input, the static calibration consists of rotating the w meter in the flow

$$[f(\omega)]^{1/2} = 0.29^\circ$$

The mechanical admittance is

$$\left| \frac{\psi(\omega)}{\psi(0)} \right| = 0.33$$

Hence, from equation (5)

$$\begin{aligned} |\phi| &= \frac{1}{\left| \frac{\psi(\omega)}{\psi(0)} \right|} \frac{[h(\omega)]^{1/2}}{[f(\omega)]^{1/2}} = \frac{1}{0.33} \frac{0.02}{0.29} \\ &= 0.21 \end{aligned}$$

for  $k = 1.95$ .

## REFERENCES

1. Clementson, Gerhardt C.: An Investigation of the Power Spectral Density of Atmospheric Turbulence. Sc. D. Thesis, M.I.T., May 1950.
2. Liepmann, H. W.: On the Application of Statistical Concepts to the Buffeting Problem. Jour. Aero. Sci., vol. 19, no. 12, Dec. 1952, pp. 793-800, 822.
3. Fung, Y. C.: Statistical Aspect of Dynamic Loads. Jour. Aero. Sci., vol. 20, no. 5, May 1953, pp. 317-330.
4. Diederich, Franklin W.: The Response of an Airplane to Random Atmospheric Disturbances. Ph. D. Thesis, C.I.T., 1954.
5. Press, Harry, and Mazelsky, Bernard: A Study of the Application of Power-Spectral Methods of Generalized Harmonic Analysis to Gust Loads on Airplanes. NACA Rep. 1172, 1954. (Supersedes NACA TN 2853.)
6. Liepmann, H. W.: Extension of the Statistical Approach to Buffeting and Gust Response of Wings of Finite Span. Jour. Aero. Sci., vol. 22, no. 3, Mar. 1955, pp. 197-200.
7. Sears, William R.: Some Aspects of Non-Stationary Airfoil Theory and Its Practical Application. Jour. Aero. Sci., vol. 8, no. 3, Jan. 1941, pp. 104-108.
8. Hakkinen, Raimo J., and Richardson, A. S., Jr.: Theoretical and Experimental Investigation of Random Gust Loads. Part I - Aerodynamic Transfer Function of a Simple Wing Configuration in Incompressible Flow. NACA TN 3878, 1956.
9. Richardson, A. S., Jr.: Theoretical and Experimental Investigation of Random Gust Loads. Part II - Theoretical Formulation of Atmospheric Gust Response Problem. NACA TN 3879, 1956.

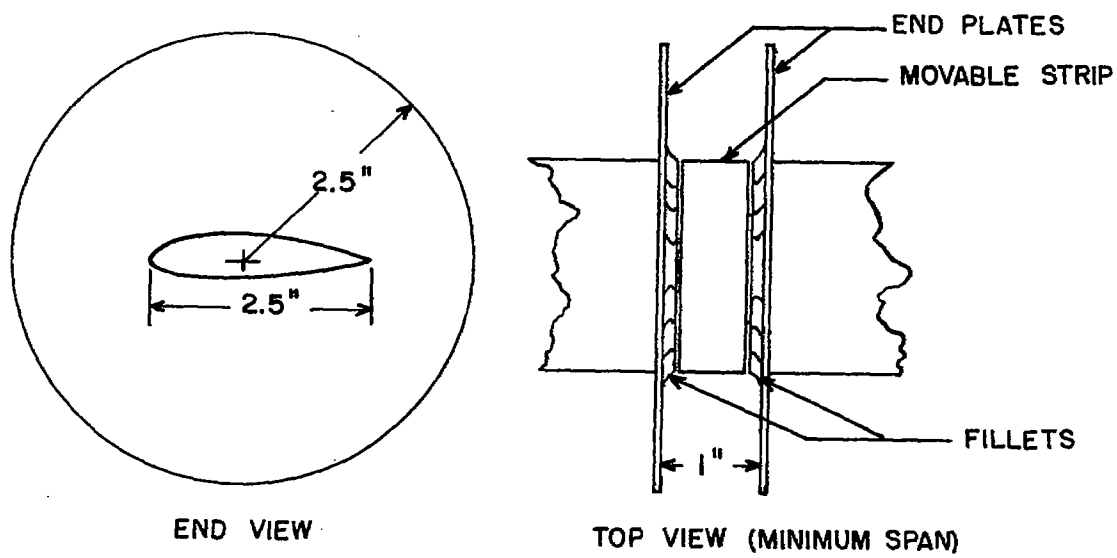


Figure 1.- Adjustable-span arrangement.

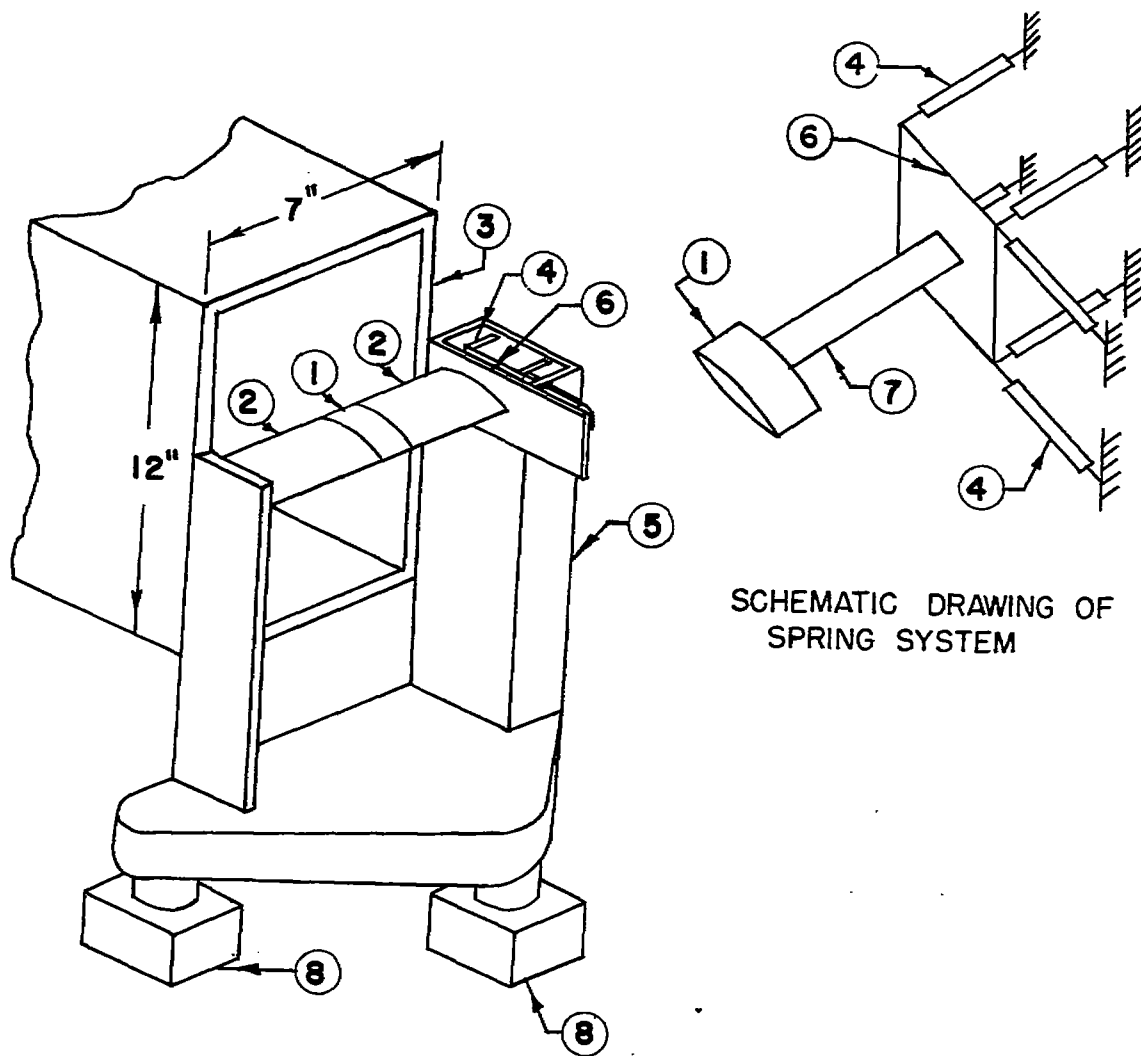
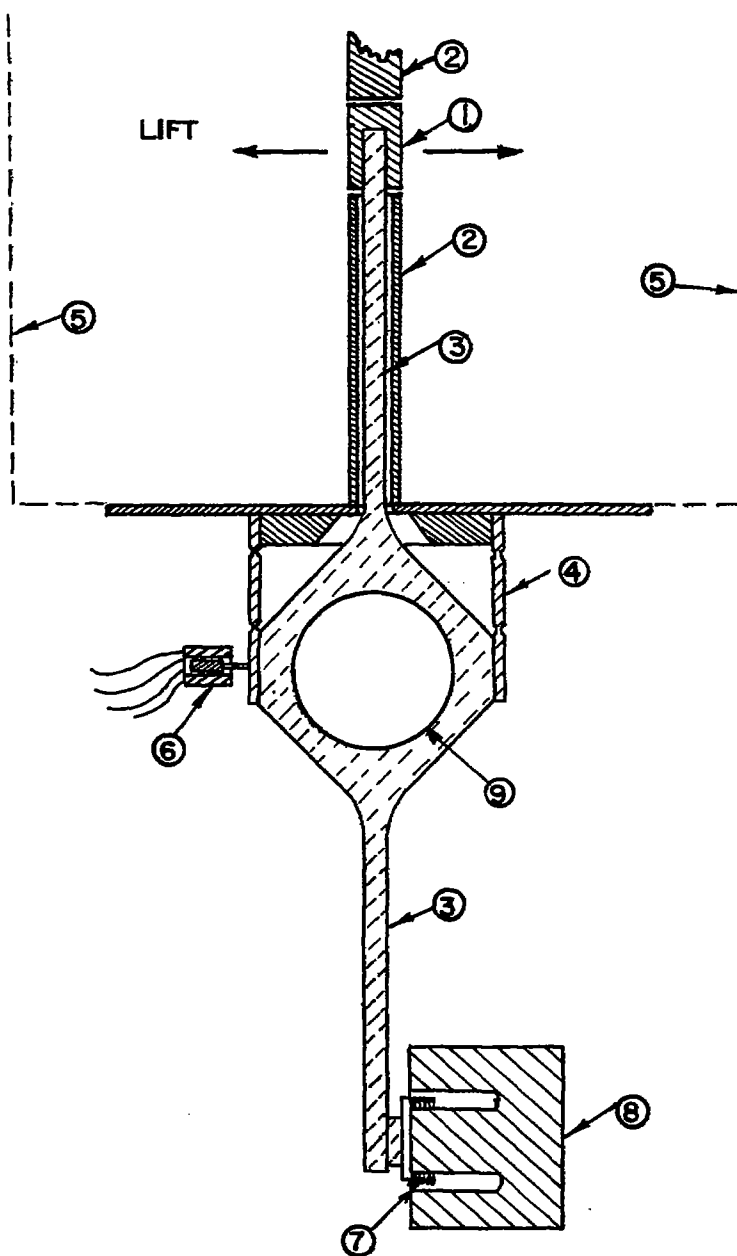


Figure 2.- Sketch of test setup in which mechanical system is used as filter. ① Movable strip; ② dummy airfoils; ③ wall of wind-tunnel jet; ④ flexure links; ⑤ steel-support structure; ⑥ location of displacement pickup; ⑦ beam; ⑧ vibration absorbers (foam rubber and paper towels).



VIEW LOOKING UPSTREAM

Figure 3.- Section view of test setup in which spring system is used as filter. ① Movable strip; ② dummy airfoils; ③ beam; ④ flexure links; ⑤ jet boundary; ⑥ Schaevitz gage; ⑦ coil; ⑧ magnet; ⑨ threaded hole for weights.

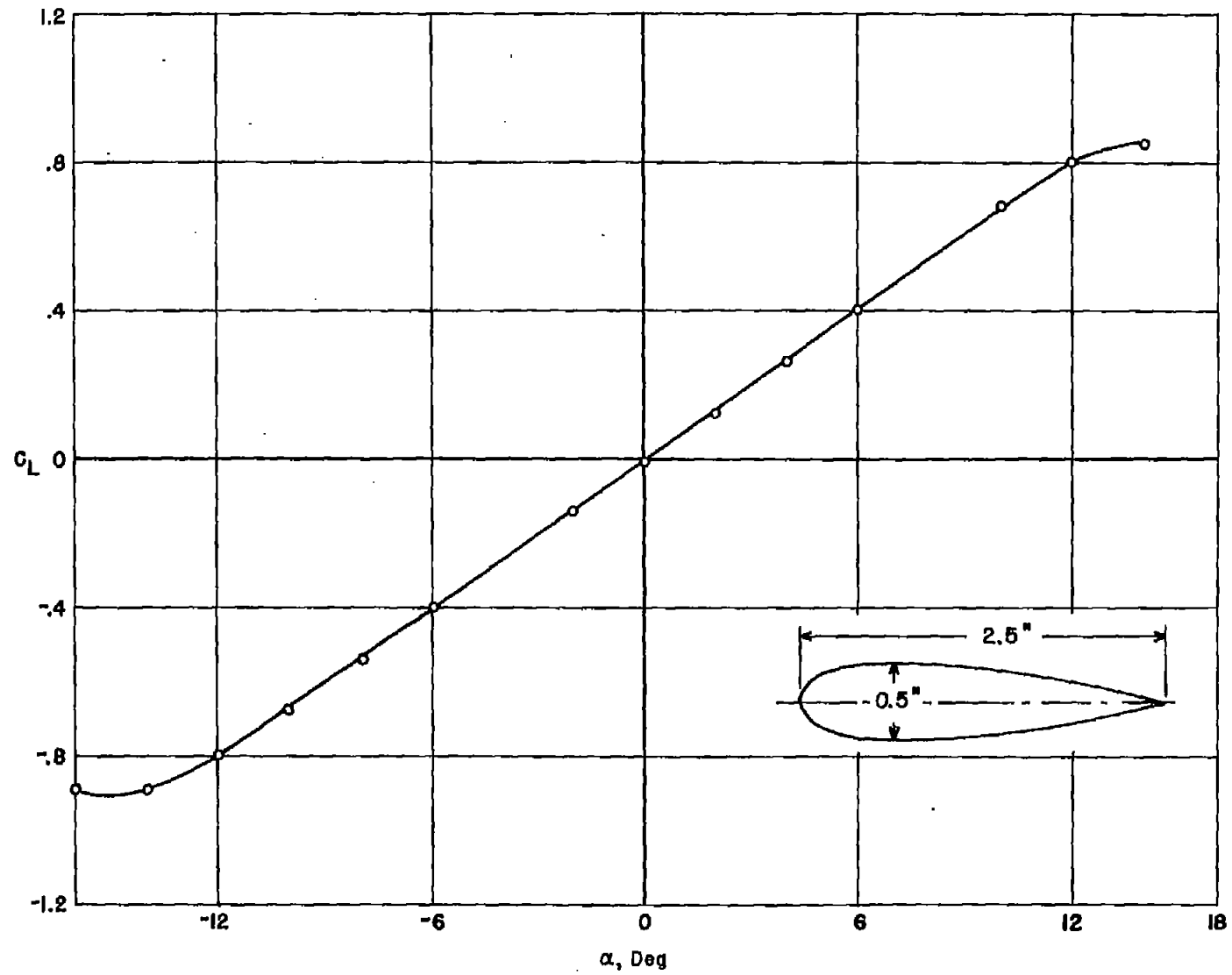


Figure 4.- Airfoil lift coefficient.  $R_e = 80,000$ ;  $C_{L\alpha} = 0.07$  per degree.

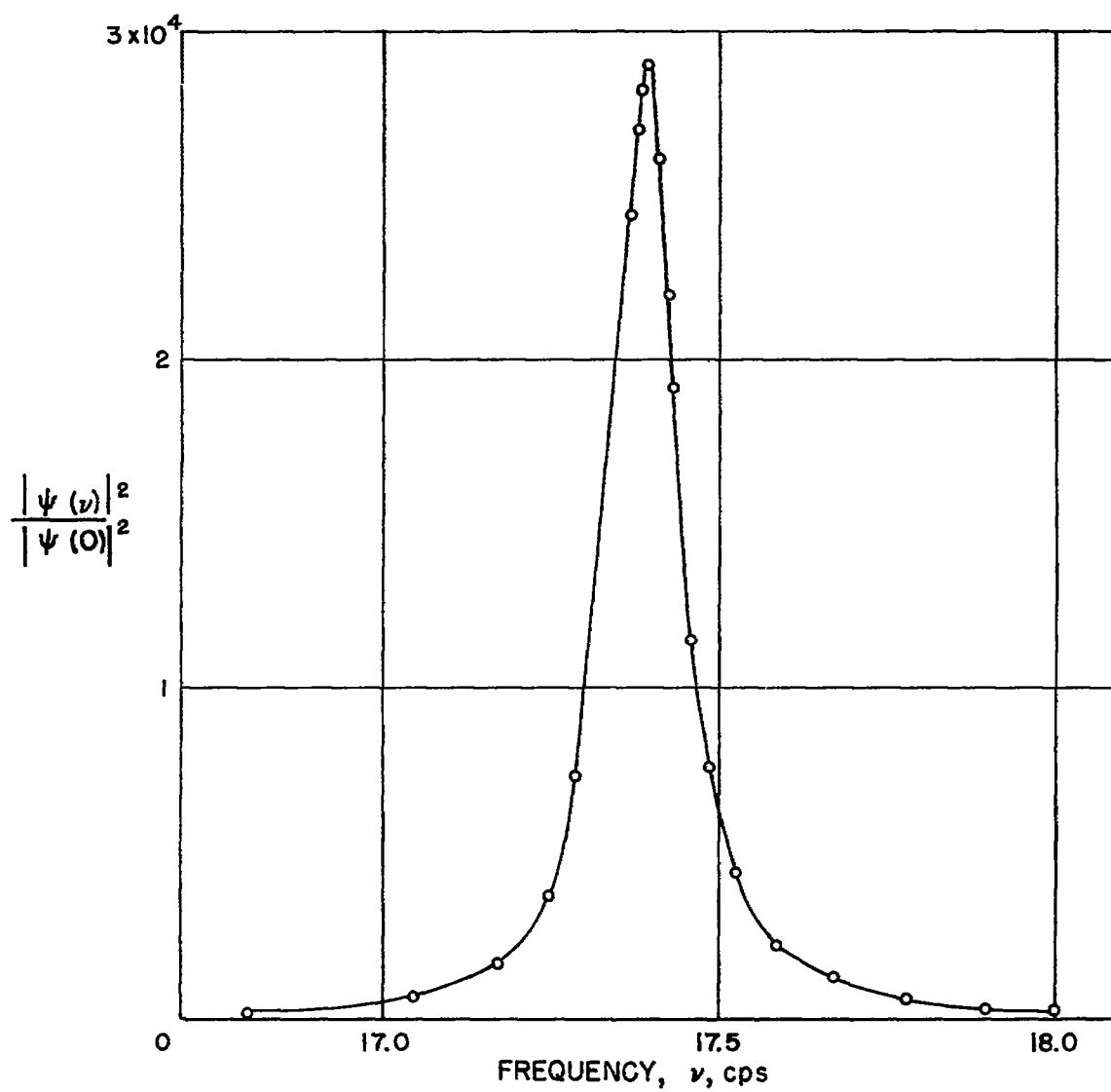


Figure 5.- Square of mechanical admittance.

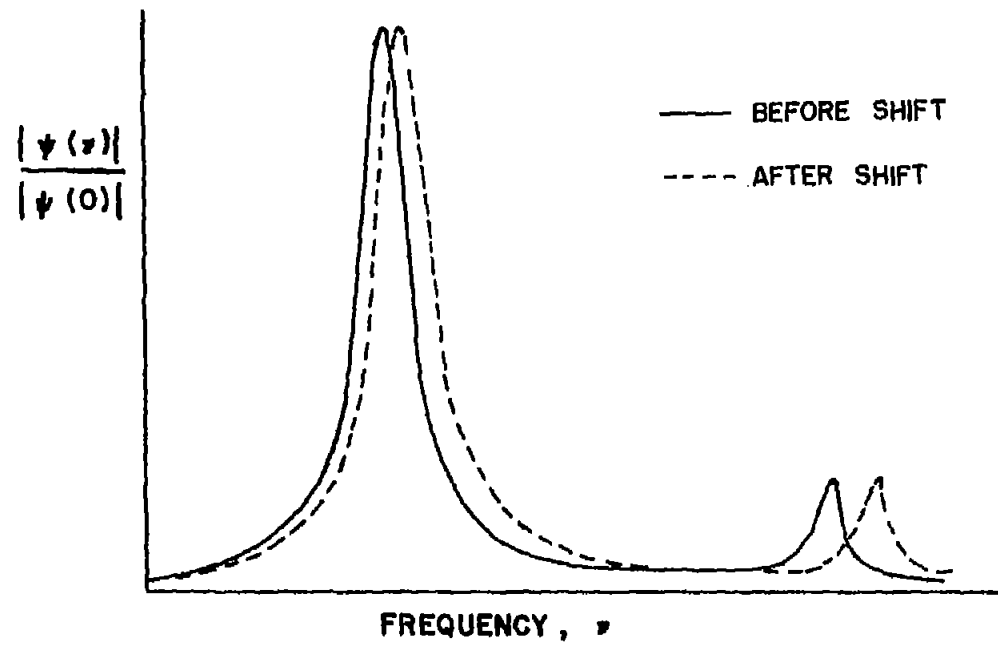


Figure 6.- Effect of frequency shift on mechanical admittance.

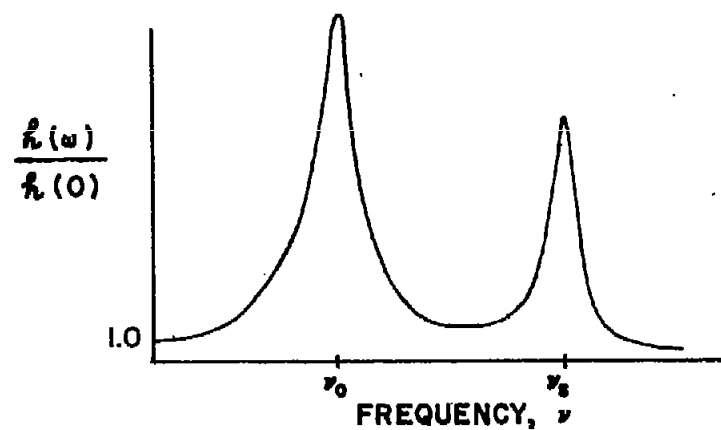


Figure 7.- Displacement spectrum for airfoil in wake of cylinder.  $\nu_0$ , natural frequency of spring system;  $\nu_s$ , shedding frequency of cylinder.

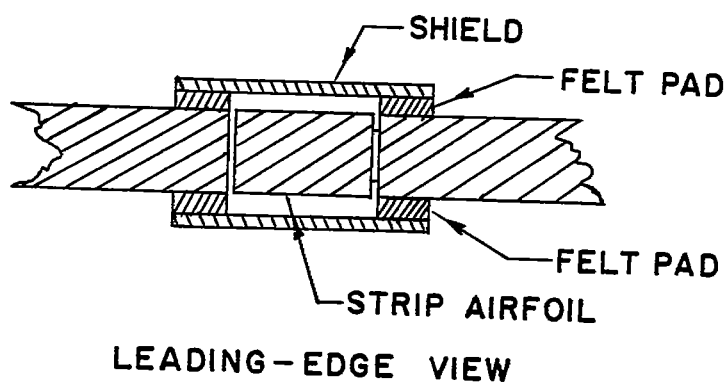
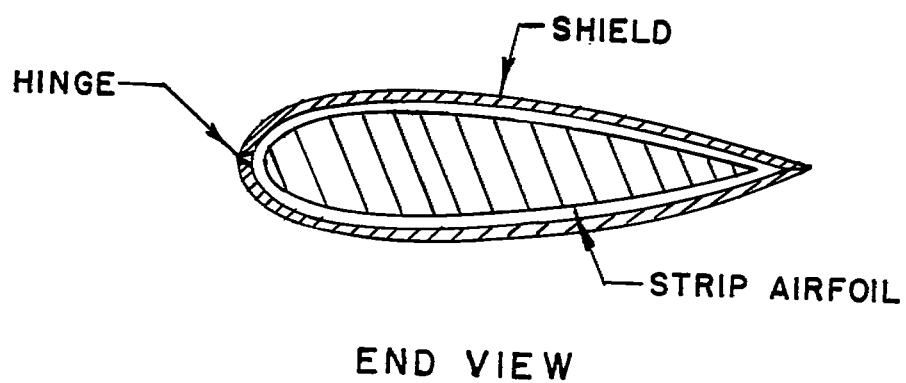


Figure 8.- Noise shielding arrangement.

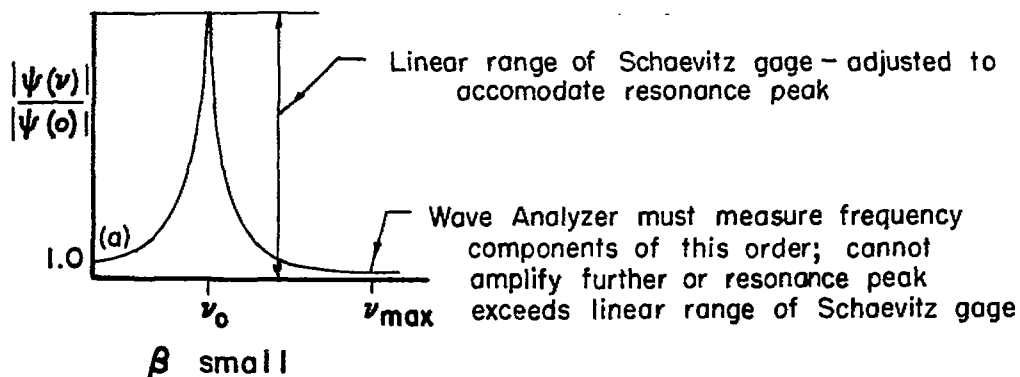
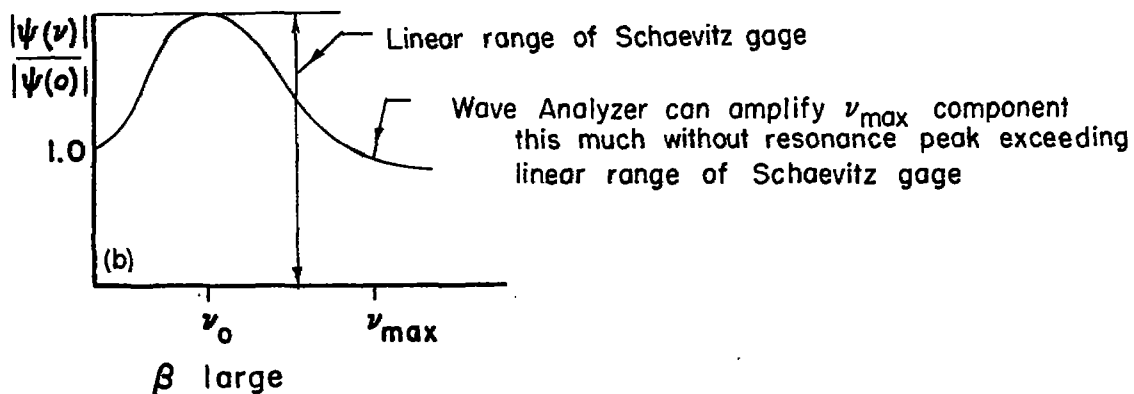
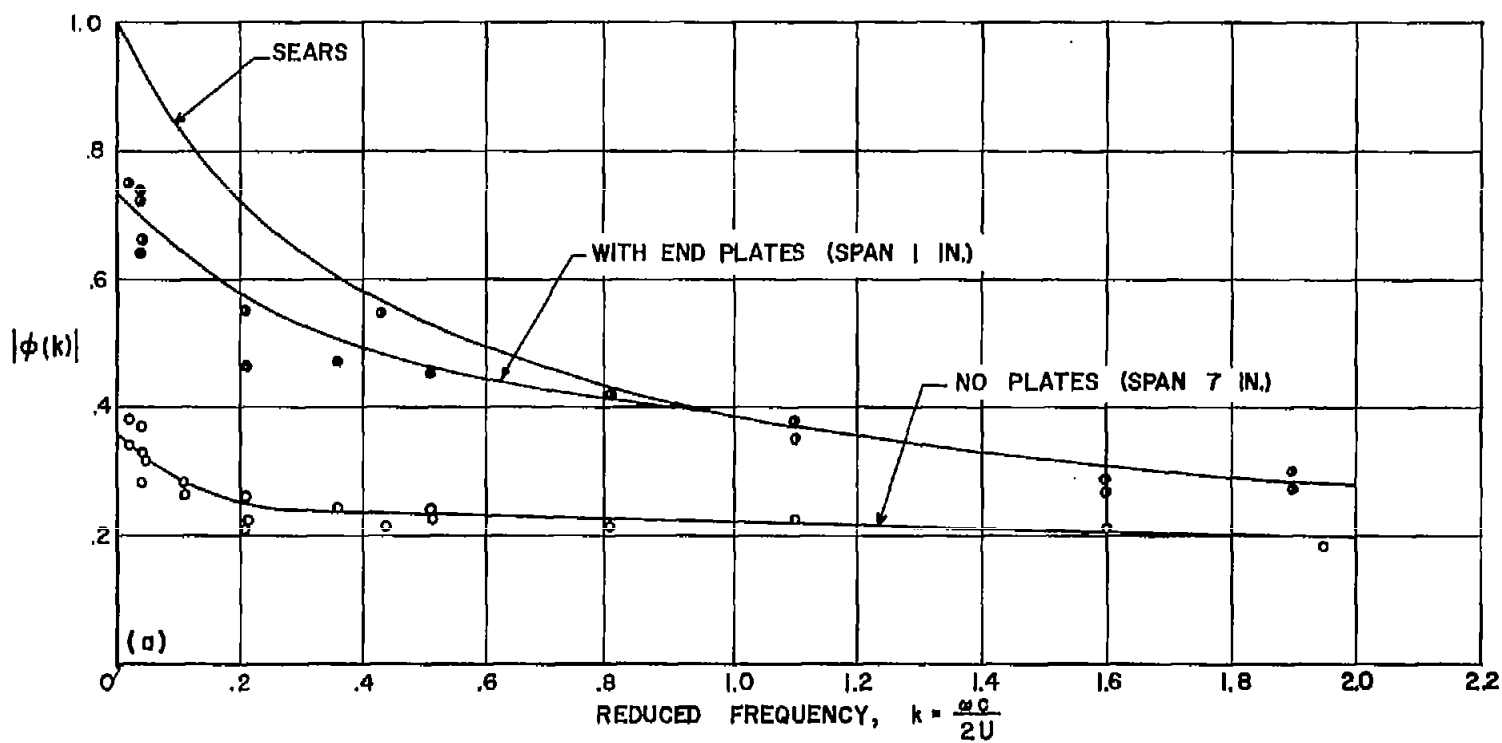
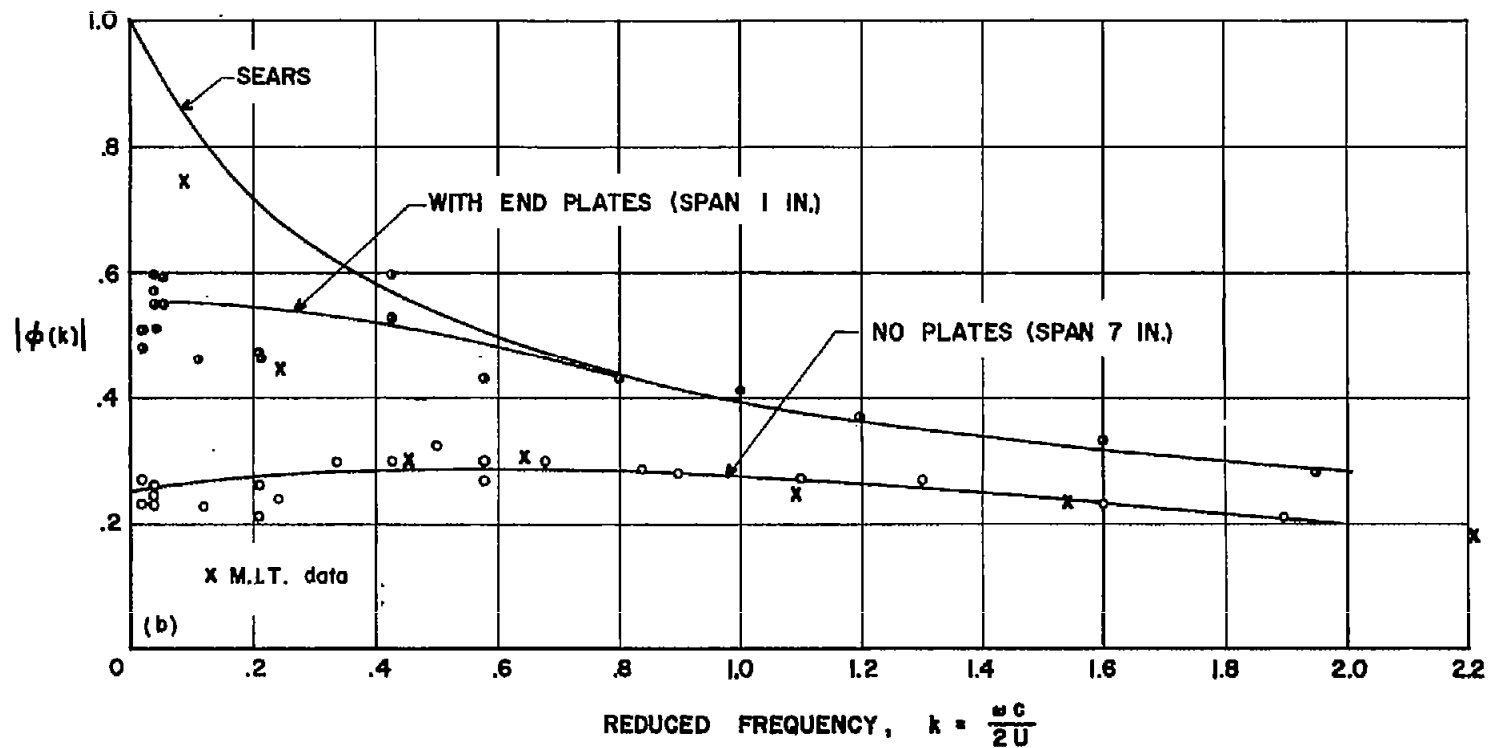
(a) Small value of  $\beta$ .(b) Large value of  $\beta$ .

Figure 9.- Spring damping requirements.



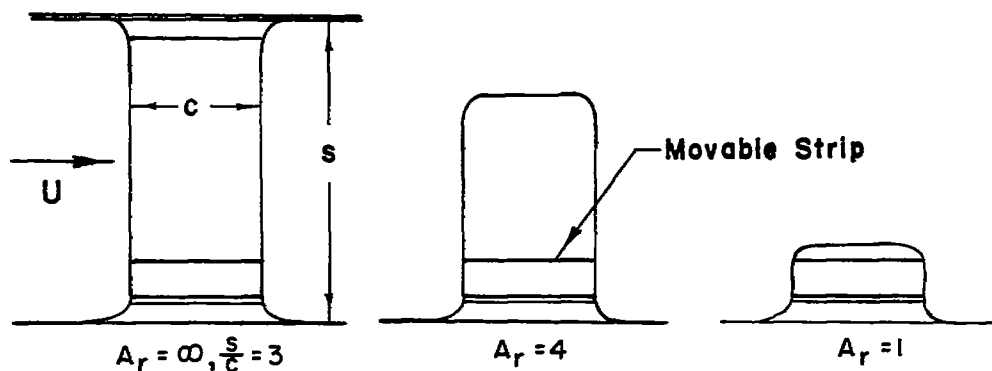
(a) Small grid ( $M \approx 1$ ,  $\frac{x}{M} \approx 20$ ,  $\lambda_x \approx \frac{1}{2}$  in.).

Figure 10.- Absolute aerodynamic admittance,  $|\phi(k)|$ .



(b) Large grid  $(M \approx 2.5, \frac{x}{M} \approx 8, \lambda_x \approx 1 \text{ in.})$ . x denotes M.I.T. data  
 (ref. 8:  $M \approx 6, \frac{x}{M} \approx 20, \frac{\text{Span}}{\text{Chord}} = 5.0$ ).

Figure 10.- Concluded.



Aspect ratio	Values of $\frac{\sqrt{L^2}}{\sqrt{L_\infty^2}}$ at -		
	Static	3 cps	17 cps
$\infty$	1	1	1
4	.89	1.25	1.48
1	.5	1.04	1.23

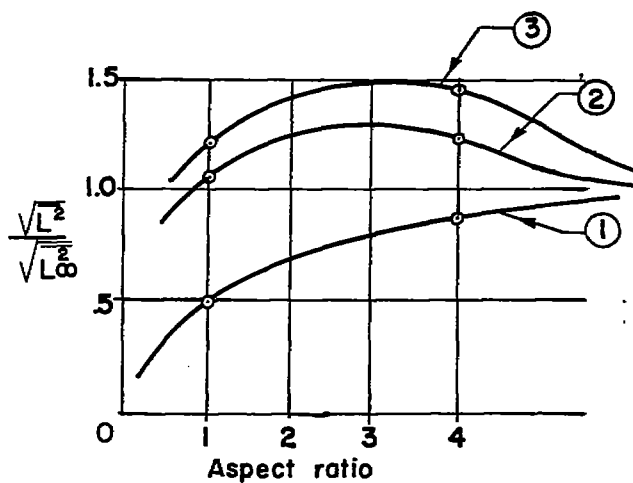
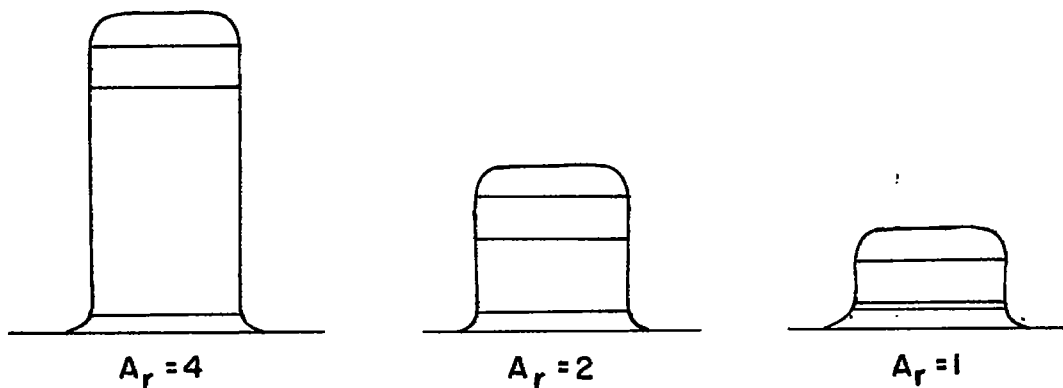


Figure 11.- Effect of aspect ratio on lift near root. ① Static response of root element; ② 3-cps response of root element; ③ 17-cps response of root element; curves approach 1.0 as  $A_r \rightarrow \infty$ ;  $\sqrt{L_\infty^2}$ , root-mean-square lift for infinite-aspect-ratio wing.



Aspect ratio	Values of $\sqrt{L^2/L_4^2}$		
	Static	3 cps	17 cps
4	1	1	1
2	.95	1.04	1.03
1	.75	1.12	1.10

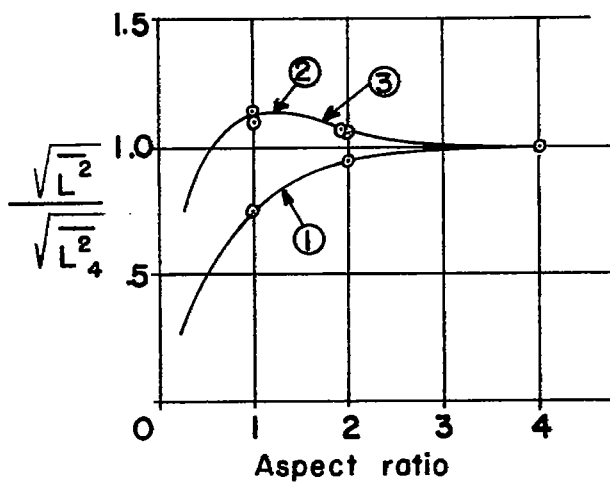


Figure 12.- Effect of aspect ratio on lift near tip. ① Static response of tip element; ② 3-cps response of tip element; ③ 17-cps response of tip element;  $\sqrt{L_4^2}$ , root-mean-square lift for wing of aspect ratio 4.